Sidelobe Analysis of BICEP3 Calibration Data

Hunter Fryman-Sinkhorn

Master's Thesis

I. Introduction

The polarization of the Cosmic Microwave Background (CMB) is our glimpse into how the universe formed. The universe began very hot and very dense, and as the universe expanded it cooled. This cooling enabled light from the early universe to escape, this is referred to as the CMB. Looking back in time to the CMB provides a view of the initial conditions of the universe. The CMB is an extremely uniform temperature 2.7K and can be seen in all directions. With a uniform temperature it implies that at the time of hydrogen recombination, roughly 3000K, the universe was uniform. The Universe is also spatially flat and based on General Relativity means it had to be even flatter in the beginning. These are the initial conditions that cosmologists are currently trying to explain. Inflation theory explains the initial conditions as it allows for the beginning of the universe to be very flat, very dense and uniform while explaining current observations. Inflation theory explains that after the Big Bang approximately 10^{-36} seconds the universe underwent rapid exponential expansion until approximately 10^{-33} seconds. This rapid expansion ensures a uniformity in the early universe to persist through to the light of last scattering and allows for a very flat and dense beginning. (Ryden 2017, Wong 2014, Chiang et al 2010)

Observing the types of polarization within the CMB could lead to confirmation of inflation. One prediction of inflation is that the universe expanding would have created density waves and gravitational waves from quantum perturbations of the inflation field and the spacetime metric respectively (Wong 2014). While the gravitational waves are too small to detect directly today, they can be detected through the polarization of the CMB. The two types of polarization in the CMB are E modes and B modes which can be best described by their orientation. (Chiang et al 2010)

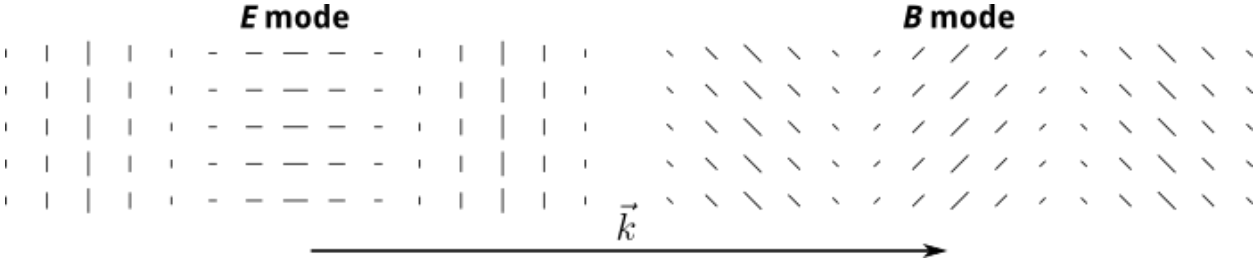

Figure 1.1 This figure shows the polarization orientation of E modes and B modes in relation to a specified direction *k.* E modes will be either parallel or perpendicular to k, while B modes will be at 45 degree angles to k. Detection of these modes in the CMB polarization, B modes in particular will provide significant evidence for Inflation theory. (Figure courtesy of C. Bischoff.)

Gravitational waves produce both E and B modes while density waves produce only E modes, therefore detecting B mode polarization in the CMB is necessary to confirm the existence of gravitational waves due to inflation.

Inflationary B modes will be on the scale of degrees, therefore observing them does not require high angular resolution. B mode polarization signal is small and the ability to obtain an accurate measurement requires low noise. The need for high precision microwave detection leads to the South Pole. The atmosphere at the South Pole is dry and thin, ideal conditions for microwave detection (Chiang et al 2010, Kaufman 2014). BICEP3 is a 520 mm aperture radio telescope with 2640 detectors designed to detect the degree scale B mode polarization in the CMB. Incredible precision is required to successfully separate the CMB B mode polarization signal (source) from noise. Eliminating systematic errors in the analysis is essential to the success of the BICEP3 project. This project focuses on an area of analysis that is one potential source of systematic error: instrument sidelobes.

II. What are Sidelobes?

With any telescope especially long wavelength telescopes, light diffraction leads to small but not insignificant sources of light that are not what the detector is pointing to. Diffraction gets harder to control at longer wavelengths such as those from the CMB. Sidelobes are defined by the collaboration as anything that is not line of sight to the detector. As an example, the electromagnetic field pattern at the aperture of the telescope can be idealized as a Gaussian distribution. The far field radiation pattern can be obtained through a Fourier transformation (See figure 2.1). This is the idealized case, the edges of the telescope will truncate the incoming electromagnetic radiation, taking the Fourier transform of the Gaussian distribution gives a visualization of the far field beam pattern of BICEP3.

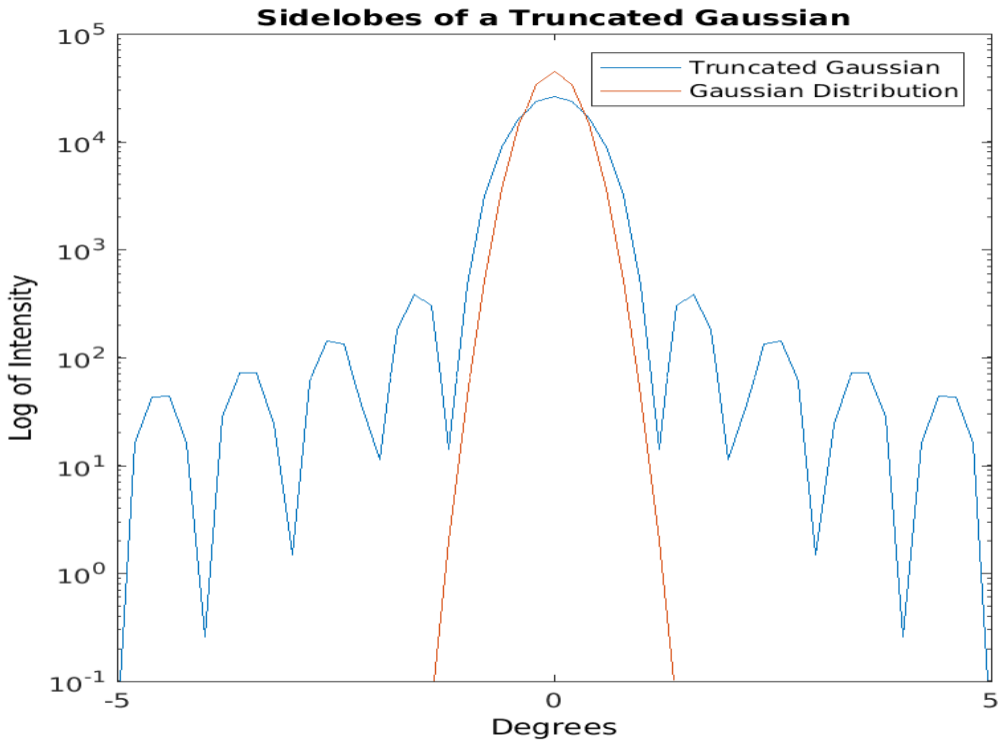

Figure 2.1 This is a one-dimensional schematic of sidelobes and the main lobe. BICEP3 is a 50cm telescope that observes at a 3mm wavelength. The orange function represents the ideal case with the blue function representing the impact of the truncation. The main lobe is what aligns with the ideal case, though with a slightly lower maximum due to the truncation. The local maxima outside of where the detector is pointing are what are referred to as sidelobes.

The "main lobe" of BICEP3 is the area of greatest field strength shown in the center of figure 2.1, the local maxima at angles outside the main beam are what are referred to as Sidelobes. The assumption is that the detector is only sensitive to what is in line of sight however significant sidelobe response is possible. If sidelobe response is present and significantly higher than the noise level, then it could be leading to systematic error in the current analysis.

In order to determine if sidelobes impact our results a calibration test is conducted. An amplified microwave calibaration source and is broadcast through a horn that is linearly polarized near BICEP3.

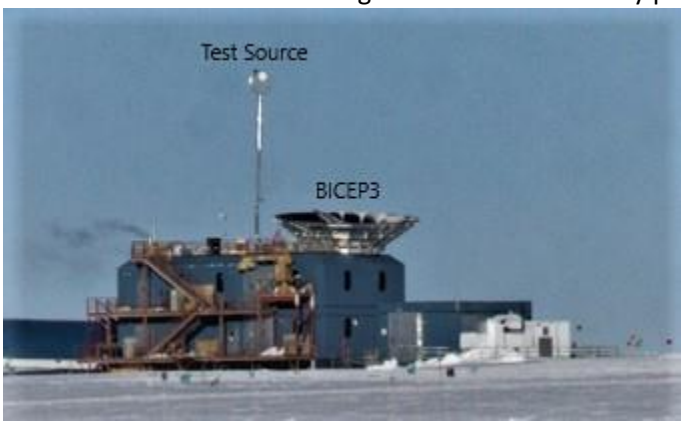

Figure 2.2 This is a photograph of BICEP3, the telescope is not visible in this picture what is shown is the ground shield around BICEP3. The test source is placed upon the mast as shown. The Telescope rotates about three axes: azimuth (az), elevation (el), and deck (dk). Deck angle is defined as rotating the telescope about the bore sight.

The test source is created by turning the source on and off at roughly 18Hz and a reference of this is recorded in the time ordered data, known as a chop reference. The telescope will rotate in azimuth by 380° after which it will rotate back to the set starting point. This is called a scan. After the scan BICEP3 will increase in elevation and repeat through its full range of motion in azimuth. The data set being analyzed includes scans over 6 different deck angles.

III. Constructing a Polarized Sidelobe Map

The overall goal of sidelobe analysis is to construct a polarized sidelobe map. This map is a pixel map of polarized detector response. The CMB can be described by the Stokes' parameters intensity (I), linear polarization (Q, U) and circular polarization (V) (Chiang et al 2010). For this project V is not utilized as the polarization of the CMB lies predominately in Q and U. The polarized sidelobe maps will be maps for Q and U polarization. In order to measure polarization BICEP3's detectors are grouped into pairs with each detector coaligned and rotated 90° in polarization angle.

Before analyzing the data, the orientation of the telescope in relation to the source must be determined. This is done to make the Q and U maps easier to read by setting the calibration source to

the origin. The angle between the source and BICEP3 is slightly different over each deck angle. If the source location is incorrect then there will be multiple source points in the map rather than one point at the origin. For each timesample the source's location with respect to where the detector is pointing needs to be constructed. The simplest solution is for a single detector to add up every time the detector visited a pixel (N) and the strength of the signal (z) for every timestream sample. Q and U are more complicated because the pair-difference data gives a linear combination of Q and U.

Adding over a set of samples "*i*" that hit a specific pixel for two parameters. ψ is the polarization orientation for each sample and d is the pair-difference data for a given detector pair. The pair-difference data is summed over two sets X and Y which are combinations of pair-difference polarization shifted 90 degrees:

$$X = \sum_i d_i * \cos(2\psi_i)$$
$$Y = \sum_i d_i * \sin(2\psi_i)$$

Expanding on what the pair-difference data is measuring

$$X = \sum_i (Qcos2\psi_i + Usin2\psi_i + noise_i) * cos2\psi_i$$

Gaussian noise averages to zero therefore:

$$< X >= Q \sum_i \cos^2(2\psi_i) + U \sum_i \cos(2\psi_i) * \sin(2\psi_i) = Q * M_{11} + U * M_{12}$$

<Y> follows a similar calculation except it is multiplied by $\sin(2\psi_i)$ instead of $\cos(2\psi_i)$

$$< Y >= Q \sum_i \cos(2\psi_i) * \sin(2\psi_i) + U \sum_i \sin^2(2\psi_i) = Q * M_{12} + U * M_{22}$$

$$\begin{bmatrix} < X > \\ < Y > \end{bmatrix} = \begin{bmatrix} \sum_i \cos^2(2\psi_i) & \sum_i \cos(2\psi_i) * \sin(2\psi_i) \\ \sum_i \cos(2\psi_i) * \sin(2\psi_i) & \sum_i \sin^2(2\psi_i) \end{bmatrix} * \begin{bmatrix} Q \\ U \end{bmatrix}$$

$$M_{11} = \sum_i \cos^2(2\psi_i)$$
$$M_{22} = \sum_i \sin^2(2\psi_i)$$
$$M_{12} = M_{21} = \sum_i \cos(2\psi_i) * \sin(2\psi_i)$$

Solving for Q and U is done by taking the inverse of the matrix and multiplying by the X and Y matrix:

$$Q = \frac{M_{22}X - M_{12}Y}{M_{11}M_{22} - M_{12}^2} \quad U = \frac{-M_{12}X + M_{11}Y}{M_{11}M_{22} - M_{12}^2}$$

Calculating variance helps provide understanding for the noise in the map:

$$var(Q) = < Q^2 > - < Q >^2$$
$$var(U) = < U^2 > - < U >^2$$

The variance calculations lead to:

$$var(Q) = \frac{M_{22}^2 var(X) + M_{12}^2 var(Y) - 2M_{22}M_{12}covar(X,Y)}{(M_{11}M_{22} - M_{12}^2)^2}$$
$$var(U) = \frac{M_{12}^2 var(X) + M_{11}^2 var(Y) - 2M_{11}M_{12}covar(X,Y)}{(M_{11}M_{22} - M_{12}^2)^2}$$

Solving for the variances requires calculating the variance in X and Y:

$$var(X) = \sum_i var(d_i) * \cos^2(2\psi_i)$$

$$var(Y) = \sum_i var(d_i) * \sin^2(2\psi_i)$$

ψ represents where the detector is pointing, and this is a known value therefore it is treated as a constant for this calculation. If there is zero noise correlation between timestream samples the variance in the pair-difference data is just σ^2. The analysis performed is with a σ^2 equal to 1 so it will not be normalized but that isn't essential to the analysis.

$$var(X) = \sigma^2 * \sum_i \cos^2(2\psi_i) = \sigma^2 * M_{11}$$
$$var(Y) = \sigma^2 * \sum_i \sin^2(2\psi_i) = \sigma^2 * M_{22}$$

The covariance calculations can be simplified when considering that each individual detector collects an independent set of data with its own gaussian noise. This means that one timestream sample is independent from other timestream samples.

$$covar(X,Y) = \sigma^2 * \sum_i \cos(2\psi_i)\sin(2\psi_i) = \sigma^2 * M_{12}$$

Substituting into the variances for Q and U yields the results:

$$var(Q) = \frac{M_{22}}{(M_{11}M_{22} - M_{12}^2)^2}$$
$$var(U) = \frac{M_{11}}{(M_{11}M_{22} - M_{12}^2)^2}$$
$$covar(Q,U) = \frac{M_{12}}{(M_{11}M_{22} - M_{12}^2)^2}$$

IV. Sidelobe Data Analysis

The analysis of the data requires three major steps: taking raw data from the telescope and demodulating it, binning the data by detector, and using the binned data to construct pair-sum and pair-difference maps for each pair of detectors.

- Demodulation

Timestream data is a measurement of detector response as the telescope moves in az, el, and dk; this does not distinguish between our desired source and the rest of the sky. Therefore, it is necessary to identify the source and separate it from all other data. This is done by demodulation. Demodulation involves reading in the timestream data, readouts of BICEP3's position information in relation to the source (sec.2), and information on the chop reference. The chop reference is cleaned up and used to

separate the timestream between data that is in phase with the chop reference and data that is out of phase with the chop reference (see figure 4.1).

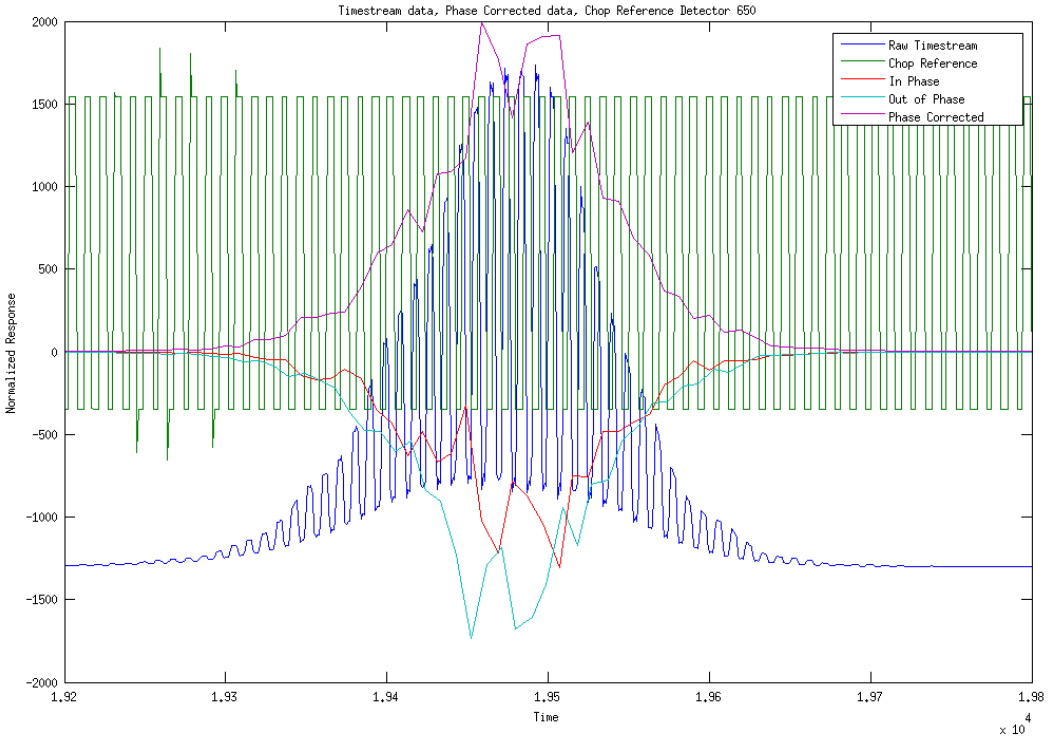

Figure 4.1: The Chop reference (in green) is shown above in relation to the timestream response for detector 650 (in blue). The raw timestream is consistent of multiple peaks and valleys that correspond to the chopping of the source. The timestream data is categorized by its two components, in phase with the chop reference (in red) and out of phase with the chop reference (in cyan). The phase corrected response is shown in purple.

Once the data is demodulated it needs to be further organized and broken down into the components necessary for analysis (see section 3). These accumulated variables are currently divided between in phase data and out of phase data based on their relation to the chop reference. The important value is the phase shift between the two data sets and calculating this phase angle, φ, is crucial to creating a polarized map. This phase angle is found by dividing the signal strength (z) by the total number of times the detector passed a specific pixel (N) for both the in phase and put of phase data sets. These are referred to as maps, and the simple Z/N maps were used to find the source location (sec.2). The in phase and out of phase data act as a cosine and sine in relation to the chop reference so taking the inverse tangent produces the phase angle between them:

$$In\ Phase\ Detector\ Map\ (m_{ip}) = \frac{z_{ip}}{N_{ip}}$$

$$Out\ of\ Phase\ Detector\ Map\ (m_{op}) = \frac{z_{op}}{N_{op}}$$

$$\varphi = \tan^{-1}\left(\frac{m_{op}}{m_{ip}}\right)$$

Once φ is found I want to cut out the φ values that are very far from the source as φ is only valuable where there is strong signal to noise (i.e. when the detector is pointed at the source). This is done by conducting a quadrature sum (referred to as ζ) of the maps. A cut is then defined as a quadrature sum for the in phase and out of phase maps (ζ) with values that are 10 times the background level, as estimated by the median:

$$\zeta = \sqrt{m_{op}^2 + m_{ip}^2}$$

$$cut = \zeta > 10 * \text{median}(\zeta)$$

$\hat{\varphi}$ is defined as the average of φ values that pass the cut. This is what is used to calculate new values for (N, Z, M11, M22, M12, a, b) that are no longer broken up by in phase and out of phase but are instead one map that is referred to as the phase shifted map.

$$z_{\hat{\varphi}} = \cos(\hat{\varphi}) * z_{op} + \sin(\hat{\varphi}) * z_{ip}$$

$$N_{\hat{\varphi}} = \cos^2(\hat{\varphi}) * z_{op} + \sin^2(\hat{\varphi}) * z_{ip}$$

$$Phase\ Shifted\ Map = \frac{z_{\hat{\varphi}}}{N_{\hat{\varphi}}}$$

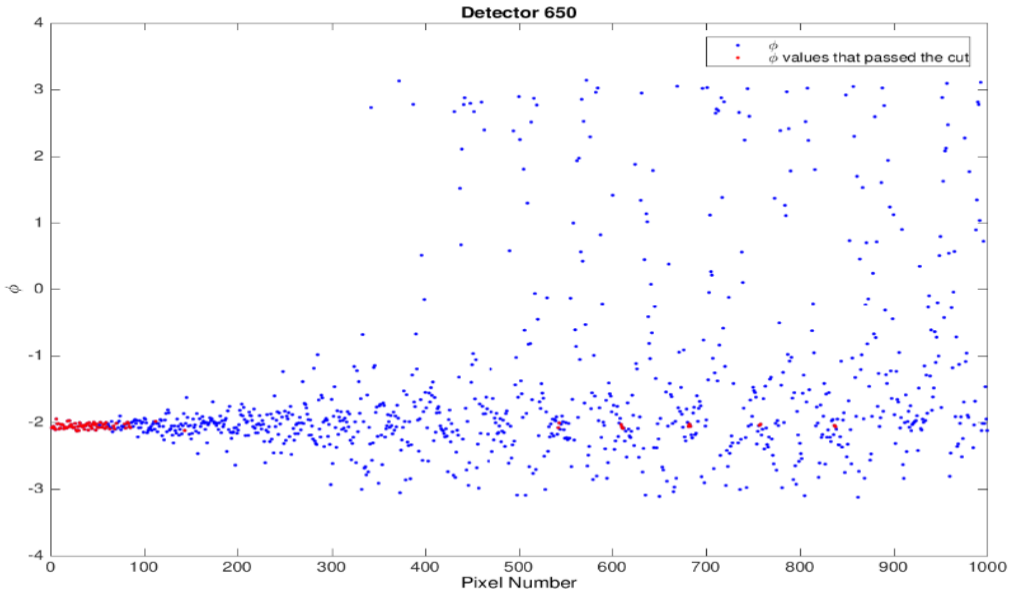

Figure 4.2: This is a plot of φ versus the first 1000 pixels out of the 49,000 total, φ values that pass the cut are marked in red. As it can be seen the majority of φ values do not pass the cut except for those near the source, pixels near zero. This is because the further away from center the pixels are the lower the signal strength is thus these outer pixels have higher uncertainty as shown by the wide range of φ values.

- Binning data by detector

Once the data has been demodulated it needs to be organized in a way that allows for the calculation of the pair-sum and pair-difference maps. First timestream data is converted from az, el and

dk into spherical coordinates (r, θ, ψ). These are not the standard spherical coordinates (ϑ, φ), in these maps r translates to distance from origin and is related to ϑ. θ is the radial angle and is the equivalent of φ. The last coordinate ψ is the polarization angle, this angle is defined as the angle between the detector's polarization axis and the source's polarization axis. The polarization angle is used to group the detectors into pairs. Each detector in a pair is rotated in polarization by 90 degrees and are labeled as "A" and "B" detectors. Then each of the values discussed in section 3 are accumulated by pixel number then binned into arrays by detector number. This accumulation is done based on the A detectors polarization angle. This is done for the polarized sidelobe maps, the A detectors have a maximum value when they are aligned with the source. This is done to determine Q and U polarization, if ψ is 0 degrees then the pair-difference will be entirely in the A detector response giving a positive result. If ψ is 90 degrees, then the signal is entirely in B response and will yield a negative result. Differentiating the two detectors is crucial to determining Q and U polarization as seen in section 3.

- Pair-sum and Pair-difference map

At the beginning and the end of each set of scans BICEP3 does what is called colloquially as an Elnod in which the telescope will increase and decrease in elevation

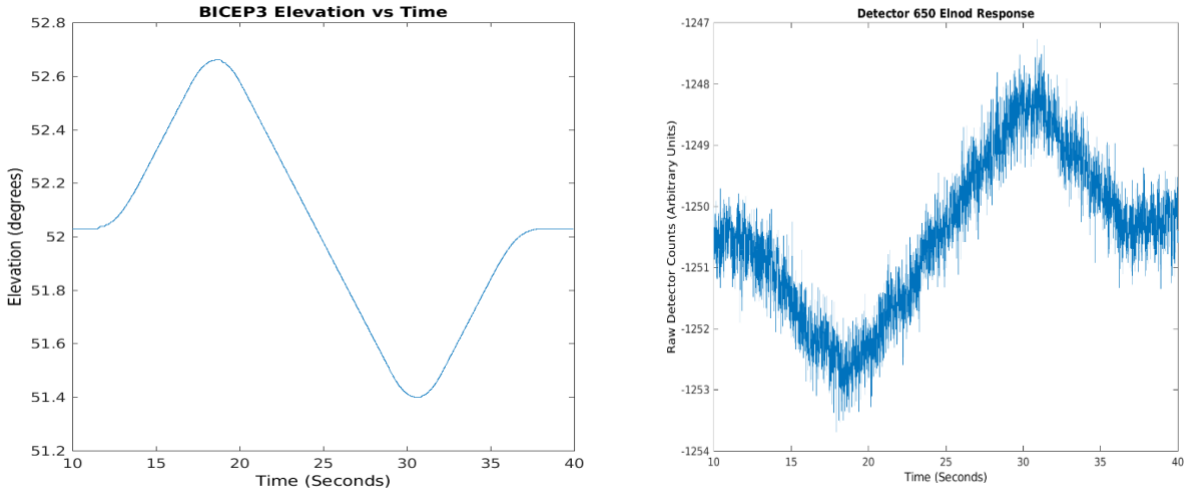

Figure 4.3 A and B: A is a track of the telescope's elevation in degrees over time in (units) compared with B which shows the detector response over the elnod. The Y axis in figure B are arbitrary units the purpose of the plot is to demonstrate how the detector responds to the change in elevation.

In order to calculate the pair-sum or pair-difference for a pair of detectors they need to first be calibrated relative to each other. This is done through the elnod. The detector pairs are separated only by their polarization angle so to calibrate them a uniform unpolarized source is needed. This eliminates the test source as it is a polarized signal, the atmosphere however is unpolarized. The atmospheric signal changes based on the elevation angle, as the elevation decreases the relative thickness of the atmosphere increases. This signal flux enables the detectors to be calibrated as a change in relative gain, referred to as Elnod Gain.

The pair-sum map is calculated by normalizing the Z and N for the A and B detectors, then summing the A and B detectors and creating a map of Z/N:

$$Elnod\ Gain\ for\ A = El_A$$
$$Elnod\ Gain\ for\ B = El_B$$

$$Z = \left(\frac{z_A}{El_A}\right) + \left(\frac{z_B}{El_B}\right)$$
$$N = N_A + N_B$$
$$Pairsum\ map = \frac{Z}{N}$$

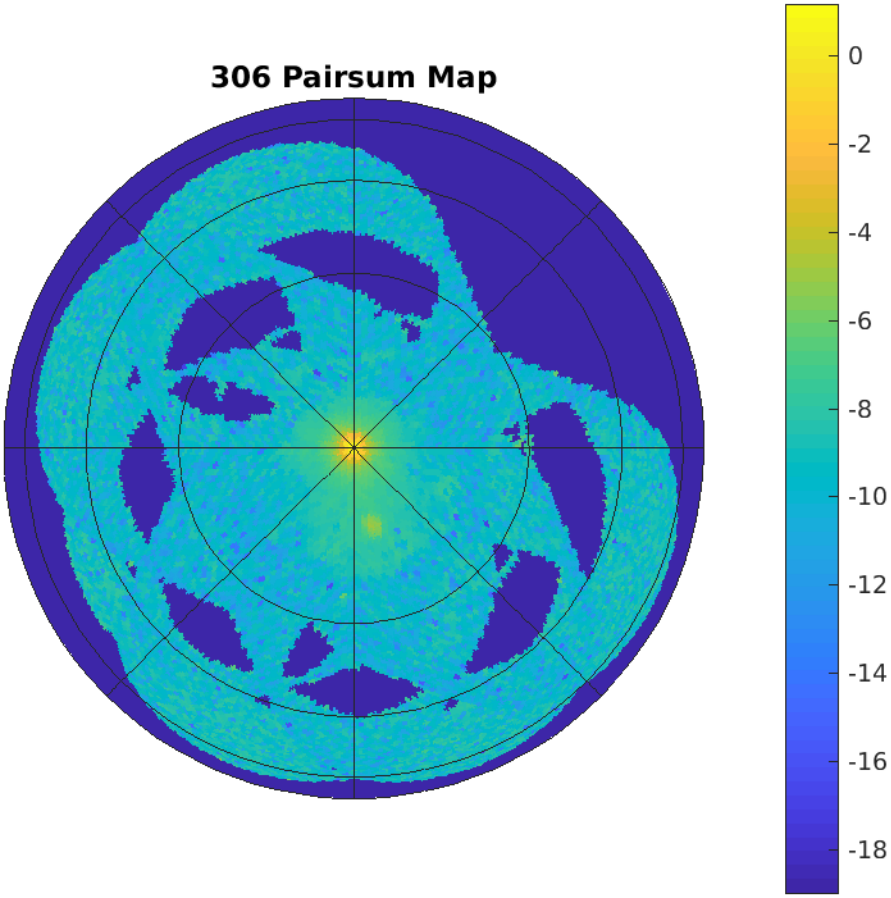

Figure 4.4: This is a map of the pair-sum signal strength divided by total response (Z/N). This map is for pair 306 which is detectors 650 and 651. When the detectors are pointing at the calibration source (0,0) is when the signal strength is at maximum, this is expected. The outer regions of the map have a lower noise floor than the single detector maps by about a factor of $\sqrt{2}$. The color scale of this map is down weighted in order to reduce the source strength as otherwise the source drowns out any potential features in the sidelobes.

In figure 4.4 the effects of a pair-sum map are seen, noise in the sidelobes reduces to a minimum. The pair-sum maps are as expected and the sidelobe data for these maps is minimal. Where the sidelobes are most likely to impact the overall results lies within the Q and U maps.

After pair-sum maps are made the next step is to construct the polarized sidelobe maps for the Q and U stokes parameters. The accumulated data and the elnod data are utilized to calculate the Q and U maps shown in section 3

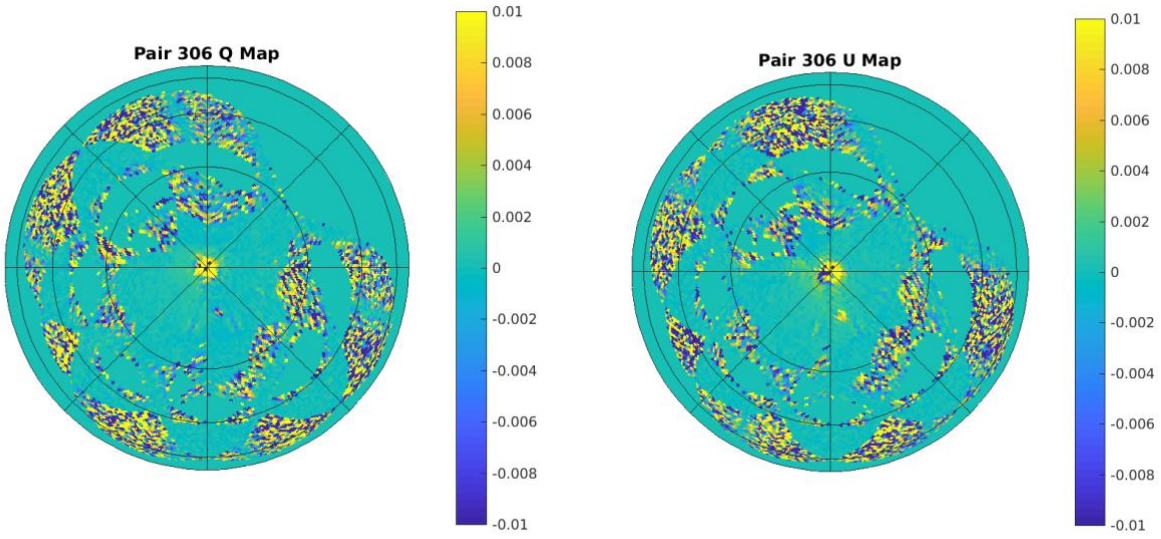

Figure 4.5 A and B: These are the Q (A) and U (B) maps for detector pair 306. The color scale is zoomed in in order to reduce the impact of the source. There is noise in the outer regions of the map areas hit by only one deck angle, shown by the regions alternating between -0.1 and 0.1. There is a region of that sits slightly above the noise floor that could potentially be a sidelobe feature seen around the source.

V. Analysis/Results

At the end of the analysis the question remains, is there sidelobe response in the Q and U maps? Yes, there are features within 20 degrees of the source but in order to determine if these features were true response and not interesting noise patterns the Q and U maps are divided by the variance in Q and U. This is intended to down weight noise and emphasize any noticeable features.

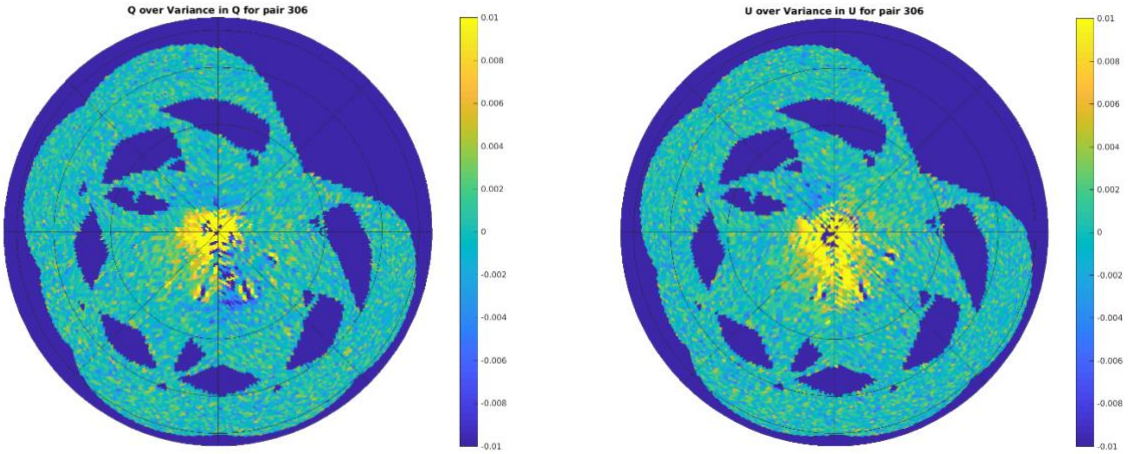

Figure 5.1 A and B: The Q and U maps after dividing by variance and after reducing the color scale to reduce source impact. Both Q and U for detector pair 306 have significant response in the 20-degree region that is well above the noise floor. The most prominent feature being the positive region around the origin having a larger angular size than the source would yield. Other smaller features are the alternating lines of positive-negative-positive values resembling a trench.

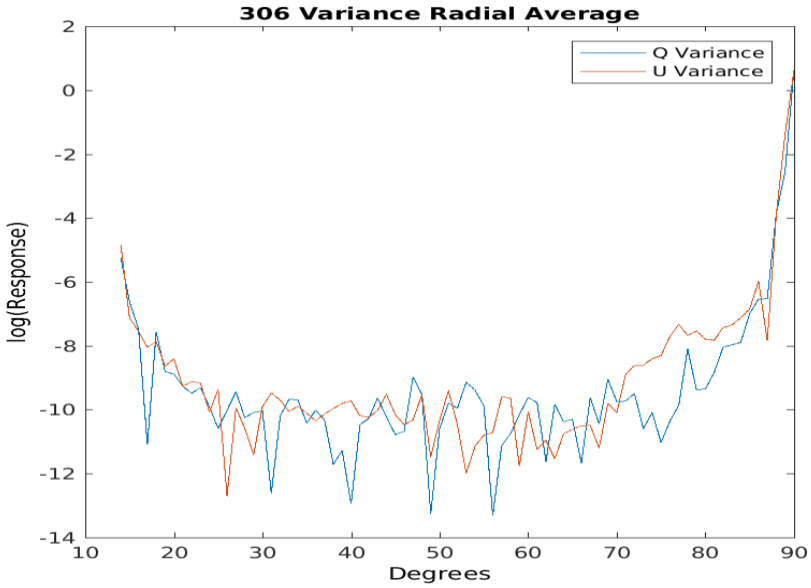

Figure 5.2: This is a 1-dimensional view of the Q (blue) and U (orange) variance maps. This plot takes the detector signal at radii ranging from 0 degrees (the equator) and 90 degrees (the origin) and takes an average from all the pixels at that radius and plots the log of the average response. The features shown in figure 5.1 can be seen within 15 degrees of the source showing that there is slightly stronger response in U than in Q. The increase in response shown near the equator is likely due to there being very few pixels leading to a higher variance.

The variance Q and U maps yielded several different features seen throughout the 1240 detector pairs. The first being the larger positive region around the source seen in figures 5.1A and 5.1B. This feature is seen in all detector pairs though the shape and sign vary throughout.

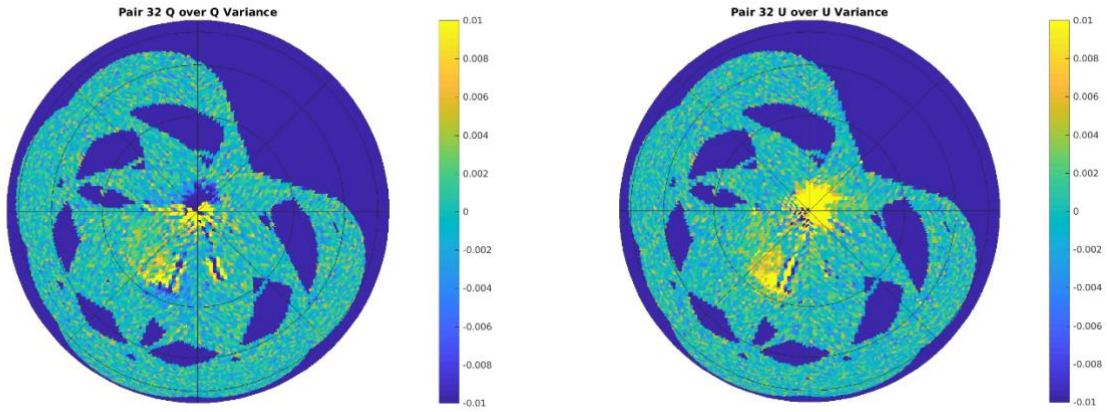

Figure 5.3 A and B: Q and U variance maps for pair 32. The region around the source has lower response when compared to Figure 5.1 with the sign in A being negative. The trench regions seen in 5.1 are more prominent in both A and B though in B only one trench appears. There is also significant response in the outer regions near the trenches

The trench like regions in nearly every map carry some consistent patterns, first any trenches appear to have an angular separation between them of 45 degrees which is the difference between deck angles. Second the trenches appear in different quadrants depending on the detector pair. Finally, detector pairs have several trenches ranging from zero to four. This points the explanation to be the pole that the source sits on. This is because BICEP3 has a limited range in elevation, the source sits at an elevation of 67 degrees meaning that when the centrally located detectors are pointed directly at the source there are some detectors pointing at the pole below it and some are pointing above. In order to ensure that every detector is pointed at the source during a scan BICEP3 is rotated in deck. This explains why different pairs see different numbers of trenches. The reason that the trenches show up in analysis is due to the nature of the chopped source. The source is chopped to help account for any features not due to the source. Demodulation should account for the pole however since the pole is thin and BICEP3 scan across it could be quick enough to not be eliminated by the chop reference. The nature of the alternating signs is due to the chop reference, the pole would look like a flat peak under normal scanning but when the source is chopped and demodulated the peak would alternate between positive and negative depending on whether the source was on or off, this can loosely be seen in figure 4.2.

In future calibration testing there are two ways to ensure that the pole does not appear in testing: Slow down the scan or speed up the chop reference. Slowing down the scan is probably not feasible given that the testing has significant time constraints and increasing scan time can have impacts on further tests. Speeding up the chop reference is a possible solution as the chop can be adjusted easily but there is an upper limit on chop frequency.

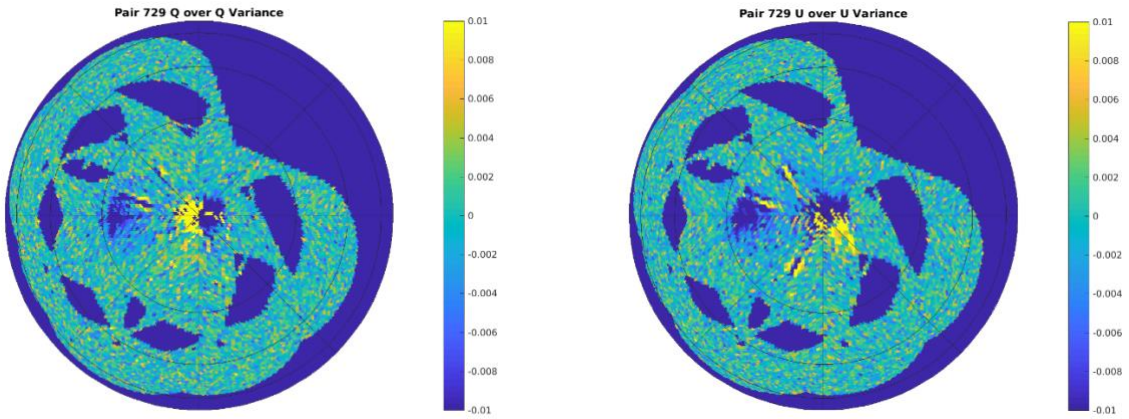

Figure 5.4 A and B: Detector pair 729 demonstrate a significant negative region out near the trenches. Also, the source is split between positive and negative regions that have differing shapes between Q and U.

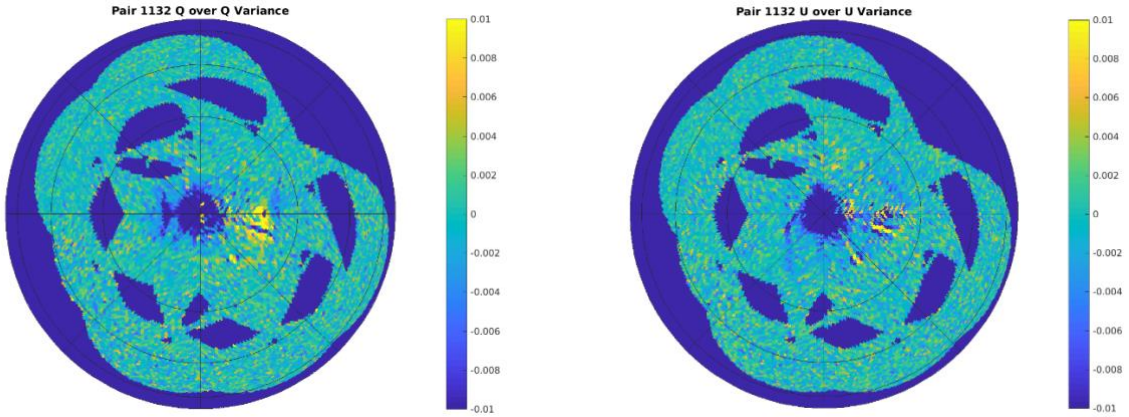

Figure 5.5 A and B: Detector pair 1132 has a negatively polarized source in both Q and U. This is interesting as only a small number of pairs show a negative response for the unpolarized source. What is expected is that the source will appear uniform throughout the detector pairs.

The positive and negative regions that do not follow the trench like pattern are areas of significant interest so they could potentially be polarized sidelobe features though further analysis is necessary to confirm.

The scope of this analysis extends beyond the limitations of this paper, further testing will be needed as this is just one set of calibration testing taking place on 2017/02/02. Calibration tests are done over different transitions, source power settings, deck angle sets, and sensitivity settings. The transition and power settings could further improve this analysis. This calibration set was done over the aluminum transition and low power. This setting allows the detectors to look directly at the source. The sensitivity in this set up is lower so that the detectors don't overload when looking at the source. Seeing the source gives better response at the origin and within 20 degrees of the source which is where the sidelobe features are seen. However, the outer regions have a higher noise floor in this setting so there

could be potential sidelobe responses beyond 20 degrees that are hidden within the noise. Running high power on the tin transition has much higher sensitivity settings but the detectors cannot look at the source. This setting will have a much lower noise floor and could detect polarized sidelobe response in the outer regions of the map. The high and low power maps could then be stitched into one complete sidelobe map providing greater insight into sidelobe response. This analysis provides the first evidence of polarized sidelobe response. Analyzing the remaining calibration set ups will be necessary to determine the scope and impact of the sidelobe response in Q and U and what the true impact is when going from calibration testing to observation.

References:

The Keck Array and BICEP Collaborations; "BK-X: Constraints on Primordial Gravitational Waves Using Planck, WMAP, and New BICEP2/Keck Observations through the 2015 Season"; Phys. Rev. Lett. 121, 221301 (2018)

Barbara Sue Ryden. (2017). *Introduction to cosmology* (2nd ed.). New York, Ny: Cambridge University Press.

Chiang, H. C., Ade, P. A. R., Barkats, D., Battle, J. O., Bierman, E. M., Bock, J. J., … Yoon, K. W. (2010). Measurement of Cosmic Microwave Background Polarization Power Spectra from Two Years of BICEP Data. *The Astrophysical Journal*, *711*(2), 1123–1140. https://doi.org/10.1088/0004-637x/711/2/1123

Kaufman, M. (2014, March 20). The South Pole Is a Great Place to View Space. Retrieved November 19, 2019, from Nationalgeographic.com website: https://www.nationalgeographic.com/news/2014/3/140319-antarctica-big-bang-inflation-telescope-south-pole-astronomy/

Maoz, D. (2007). *Astrophysics in a Nutshell*. Princeton Princeton University Press.

Wong, C. L. (2014). *Beam Characterization and Systematics of the BICEP 2 and Keck Array Cosmic Microwave Background Polarization Experiments*.